Journal of the European Ceramic Society **15** (1995) 343–348
1995 Elsevier Science Limited
Printed in Great Britain
0955-2219/95/$9.50

Effects of Composition Changes on the Crystallization Behaviour and Properties of SiO_2–Al_2O_3–CaO–MgO (Fe_2O_3–Na_2O–K_2O) Glass-Ceramics

V. K. Marghussian & M. H. Dayi Niaki

Ceramics Division, Department of Materials Science, Iran University of Science & Technology, Narmak, Tehran, Iran

(Received 4 December 1993; revised manuscript received 10 June 1994; accepted 28 July 1994)

Abstract

Several glass-ceramic materials located in the SiO_2–Al_2O_3–CaO–MgO(Fe_2O_3–Na_2O–K_2O) system were formulated by using naturally occurring materials and 1 wt% chromite ore as a nucleant. The crystallization behaviour of specimens was investigated by using dilatometric, DTA and XRD techniques. It was found that the replacement of CaO by MgO has a profound effect on the crystallization behaviour of specimens and some of them show almost complete crystallization. After a two stage heat treatment, an aluminium dioxide phase was identified as the sole crystallization product in all specimens. The microstructures were investigated by SEM.

It was found that phase separation occurs prior to nucleation of dioxide and the latter phase grows into a fibrous shape. The bending strength of crystallized specimens which range from 31 to 76 MPa depends on the degree of crystallinity and on the porosity of specimens. The hardness and chemical durability values depend only on the amount of crystalline phase.

1 Introduction

Glass-ceramic materials which are produced by controlled nucleation and crystallization of glass have received considerable attention in recent years. Among various glass-ceramic materials those of the SiO_2–Al_2O_3–MgO–CaO (Na_2O,K_2O,Fe_2O_3) system are mainly produced from inexpensive natural or synthetic materials such as blast furnace slags,[1–4] basalts,[5–7] oil shales,[8] granite and tuff.[9]

In the present work, an Iranian andesite rock was used as the main constituent to produce a glass-ceramic material and the effect of compositional changes was investigated. All the chosen compositions were part of the system mentioned above.

2 Experimental Procedure

2.1 Starting materials

Local materials, namely andesite rock from the Goorid mine, Birjand (North East Iran), quartz sand from Ghezel-Ghiyeh, magnesite from Birjand, limestone from Boroojerd and chromite from Faryab were used for glass batch preparation. Six batch compositions were selected for study. The chemical compositions of the raw materials and their resultant glasses are given in Tables 1 and 2 respectively.

2.2 Melting and forming

The batch materials were ground into a fine powder, (-60 mesh for all batches, except chromite which was -200 mesh) and after mixing thoroughly were put into preheated fire clay crucibles and melted in an electric furnace at 1300°C for 3–4 h. The melts, which were homogeneous and bubble free, were then cast into stainless steel moulds. The moulds were previously preheated at 440°C which was calculated according to the Coenen procedure.[10]

The glassy specimens (14 × 2 × 1·5 cm) were then properly annealed at the 'annealing temperature' (T_g+5) for 30 min.

2.3 Heat treatment procedure

Differential thermal analysis (DTA) and dilatometric techniques were used in order to follow the changes occurring during the heating of the specimens and thus to determine the suitable nucleation and crystallization temperatures. Differential

Table 1. Chemical compositions of raw materials wt%

Oxide	*Andesite rock*	*Quartz*	*Limestone*	*Magnesite (calcined)*	*Chromite*
SiO_2	63·28	96·62	1·95	0·85	3·52
Al_2O_3	16·15	1·99	—	0·43	9·39
TiO_2	0·76	—	—	—	—
Fe_2O_3	4·12	0·092	0·26	0·07	14·78
CaO	4·38	0·58	54·33	7·79	—
MgO	1·47	0·14	—	90·21	16·97
Na_2O	3·78	0·14	—	—	—
K_2O	3·34	0·21	—	—	—
Cr_2O_3	—	—	—	—	51·13
L.O.I.	2·68	0·25	43·45	0·65	4·21

Table 2. Chemical compositions of prepared glasses[a] wt%

Oxide	*Glass A*	*Glass B*	*Glass C*	*Glass D*	*Glass E*	*Glass F*[b]
SiO_2	50·05	50·05	50·05	50·05	50·05	50·05
Al_2O_3	12·38	12·38	12·38	12·38	12·38	12·38
TiO_2	0·58	0·58	0·58	0·58	0·58	0·58
Fe_2O_3	3·18	3·18	3·18	3·18	3·18	3·18
CaO	27·21	24·71	22·21	19·71	17·21	14·71
MgO	1·29	3·79	6·29	8·79	11·29	13·79
Na_2O	2·75	2·75	2·75	2·75	2·75	2·75
K_2O	2·56	2·56	2·56	2·56	2·56	2·56

[a] 1 wt% Chromite was added to all batches.
[b] Later omitted due to its incomplete melting.

thermal analysis was made in the range 20 – 1100° using powdered samples together with powdered alumina as an inert reference material. The rate of heating in DTA and dilatometer was 10°C/min and 5°C/min, respectively.

Each glassy sample was held at its appropriate nucleation and crystallization temperatures (as determined by DTA and dilatometric techniques) for 3 h.

The heating rate was 10°C/min up to the nucleation temperature and 1°C/min between nucleation and crystallization temperatures.

2.4 X-Ray Diffraction (XRD) and microscopic examinations

The crystallized samples resulting from any of the above mentioned heat treatment schedules were then subjected to XRD and microscopic studies, using a scanning electron microscope (SEM).

2.5 Determination of the physical and chemical properties

The bending strength, micro hardness, density, porosity and chemical durability of the crystallized samples were determined.

3 Results and Discussion

3.1 The crystallization behaviour of glasses

Table 3 shows the glass transition temperatures

Table 3. T_g and T_d values

Specimen	T_g°C	T_d°C
A	663	720
B	660	720
C	657	715
D	655	700
E	653	700

(T_g) and dilatometric softening points (T_d) for glasses A – E. A typical dilatometric curve, represented in Fig. 1 shows the exact locations of T_g and T_d. It can be concluded from Table 3 that by increasing the content of MgO at the expense of CaO, a gradual decrease in both temperatures has occurred. This can be attributed to the gradual decrease of viscosity due to the replacement of CaO by MgO.

Figure 2 gives a typical DTA curve. An endothermic peak is observed beginning at 657°C (T_g) and reaching a maximum at 715°C (T_d), which can be attributed to the glass transition.

The exothermic dip centred at about 915°C is associated with the crystallization of glass. The suitable nucleation temperature (T_n) is usually taken in the 'nucleation range', between T_g and T_d.

The T_n values were determined using 'trial and error', which consisted of holding the specimens at various temperatures within the nucleation range in a gradient furnace, followed by a second hold at 'crystallization temperature' and observing the appearance of specimens. Afterwards, it was found that T_n values determined in this way can also be located approximately at the point where a distinct slope change appeared in the endothermic 'hill' in the DTA curve (Fig. 2). This was later proved to be associated with glass in glass separation.

It is interesting to note the T_n values determined from DTA traces may be fitted into an approxi-

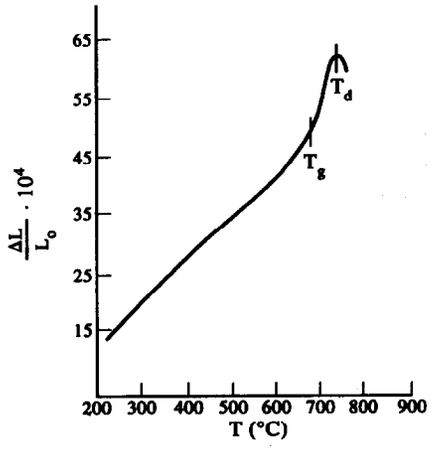

Fig. 1. Dilametric expansion curve of specimen C showing T_g and T_d values.

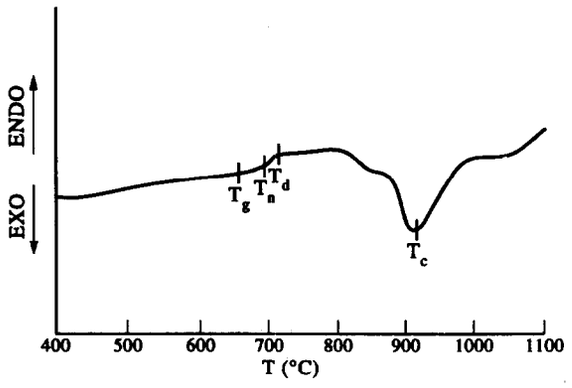

Fig. 2. DTA trace of specimen C showing, T_g, T_d, T_n and T_c values.

mate formula which relates the T_n values to the values to the glass transition and dilatometric softening points:

$$T_n = T_g + \frac{2}{3}(T_d - T_g). \quad (1)$$

Table 4 shows the nucleation and crystallization temperatures for glass samples. The gradual decrease of crystallization temperatures can also be related to the drop in viscosity caused by compositional changes.

3.2 XRD analysis

X-ray diffractometry performed on various heat treated specimens showed that an aluminium dioxide with a pattern very similar to 'Fassaite', Ca $(Mg_{0\cdot8}Al_{0\cdot2})$ $(Si_{1\cdot8}Al_{0\cdot2})O_6$ is the sole crystalline phase observed in all specimens. Regarding the compositions of glass samples, it is likely that some Fe, Na and K have also been substituted in the crystal structure (mainly for Ca). Figure 3 gives the XRD patterns for all specimens. Sample A obviously shows no sign of crystallization and exhibited only slight surface crystallization.

A quantitative X-ray analysis was performed according to the Ohlberg and Stickler method,[11] later revised by Kim *et al.*[12] Figure 4 presents the crystallization results. The amount of crystalline phase rises (Sample B to C), then drops (Sample C to D), finally rising to a very high value (95%). This behaviour can be attributed to competing

Table 4. The nucleation and crystallization temperatures

Specimen	*Nucleation temp from DTA* (T_n)°C	*Nucleation temp Calculated from Eqn. (1)* °C	*Crystallization temp.* °C
A	700	701	920
B	700	700	918
C	693	696	917
D	690	685	910
E	685	684	906

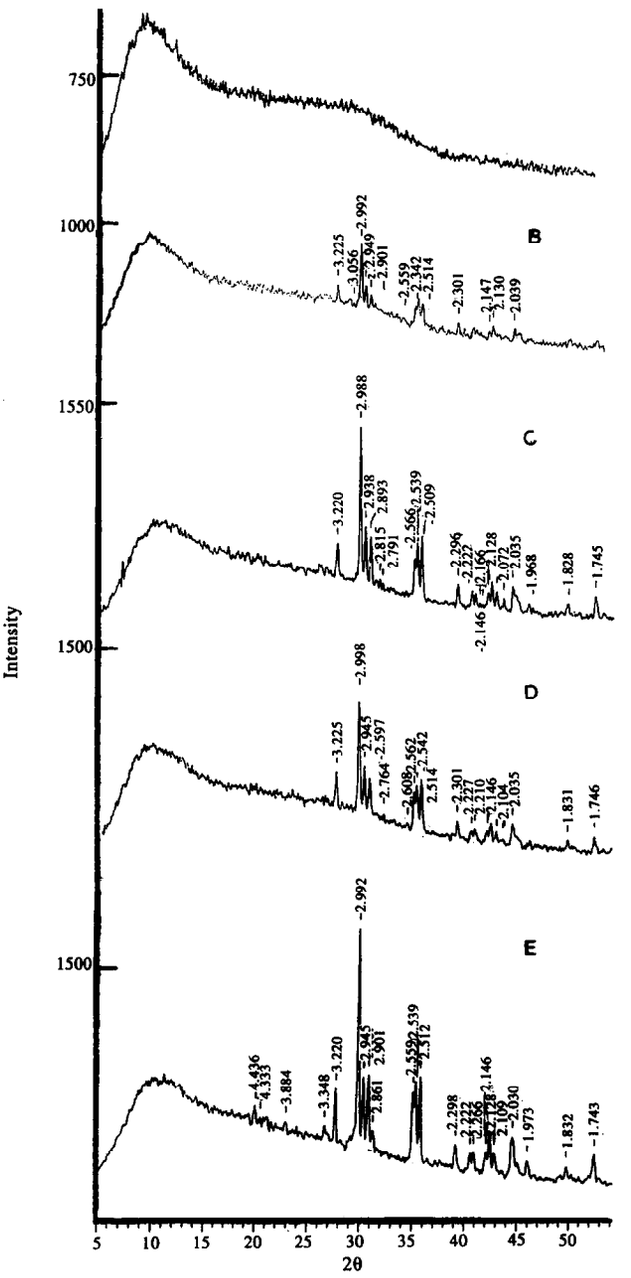

Fig. 3. XRD traces of specimens A to E.

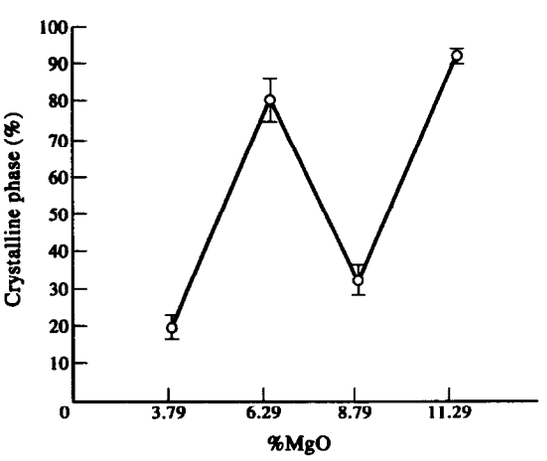

Fig. 4. Percent crystallinity versus composition (wt%).

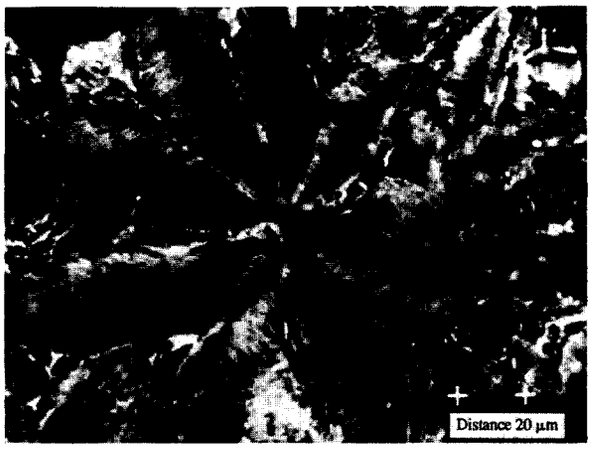

Fig. 5. SEM micrograph of specimen C showing flower-like crystalline aggregates (polished and etched in 2% HF for 5 min.)

thermodynamic and kinetic factors. As was stated previously, the viscosity decreases as a result of replacing CaO by MgO. This increases the crystallization rate. The liquidus temperature is another factor which can affect the crystallization behaviour. The rise of liquidus temperature enhances the crystallization and its drop favours the glass stability. It can be concluded therefore, that the liquidus temperature has probably increased from Specimen B to C and D to E (or if it has decreased the effect of viscosity has predominated), whereas from Specimen C to D the liquidus temperature has dropped. In addition to these factors which affect the growth process, other factors relating to nucleation, such as the effect of composition on surface tension or phase separation, may also be involved.

3.3 Microscopic examinations

Figure 5 shows the micrographs taken by SEM from polished and etched crystallized specimens. The specimens exhibit a special type of dendritic growth giving rise to flower-like crystalline collections. The microstructures of various specimens

Fig. 6. SEM micrograph of glass C after a 3 h hold at nucleation temperature showing extensive phase separation.

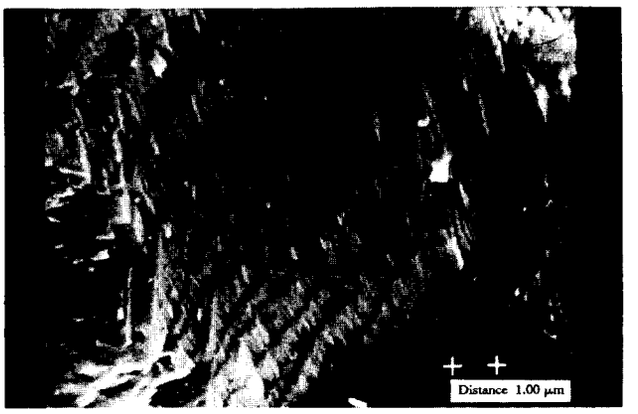

Fig. 7. SEM micrograph of glass C after crystallization showing fibrous morphology of dioxide crystals.

were also studied by SEM using fractured surfaces. Glassy samples which immediately after forming were annealed, did not show any sign of phase separation and inhomogenity up to a magnification of 300 000.

Figure 6 shows that after 3 h hold at the nucleation temperature the glassy sample has became highly phase separated. This observation is in agreement to findings of other investigators.[8,13]

According to McMillan,[13] "chromium in the Cr^{6+} state, being an ion of high field strength is likely to occupy an interstitial position and exert a marked 'ordering' effect upon its surrounding oxygen ions. Under these circumstances a chromium rich phase would separate out from the glass". A mixed spinel of formula $(Mg,Fe)(Al,Fe,Cr)_2O_4$ is then crystallized within the chromium rich phase and acts as a nucleant inducing the crystallization of dioxide.[8] It is likely that the above mentioned nucleation mechanism is also operative in the present investigation, although it was not possible to observe and identify the actual nucleating agents. Figure 7 shows the SEM micrograph of crystallized C glass.

It can be seen that the 'flower like' crystalline collections are themselves composed of 'thread like' fibrous aggregates which have grown in parallel orientation.

The fibrous aggregates consist of tiny, elongated crystals of dioxide, having about 1 μm average length and 0·1 μm average width. These crystals have grown parallel to each other in a direction which makes an angle of about 55–60° with the major axis of 'threads'.

3.4 Mechanical properties

Figure 8 gives the results of three point bending test which was carried out according to ASTM procedure C 158-84 over a span of 10 cm in bars (12 × 2 × 2 cm) cut roughly from original specimens and then ground to size. Each point represents

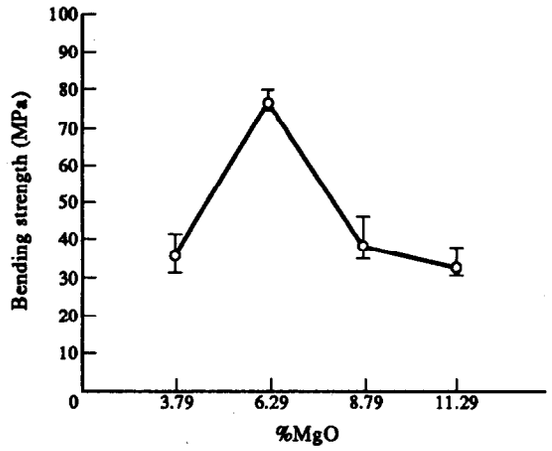

Fig. 8. Bending strength values as a function of composition (wt%). (Each point represents the average value for 10 specimens).

the average value for ten specimens.

It can be concluded that the main factor contributing to the bending strength is the amount of crystalline phase. The relatively low value for Specimen E, in spite of its very high crystallinity, can be attributed to it relatively high value of porosity (see Table 5). It seems that the porosity is mainly formed at the final stage of crystallization. At this stage, the lack of sufficient glassy phase to fill the gaps resulting from crystallization (due to a difference between densities of glassy and crystalline phases) leads to formation of some porosity. The viscous flow of glassy phase at the earlier stage of crystallization, results in pore filling and overall shrinkage of specimens without any considerable pore formation. Our calculations showed that the density of glassy specimens were in the range 2·67–2·69 Mgm^{-3} whereas the mean density of crystalline phase was 3·15 Mgm^{-3}.

From Fig. 9 which shows the knoop hardness values of various specimens, it can be concluded that with increase of crystallinity, the hardness values were also increased. (The hardness tests

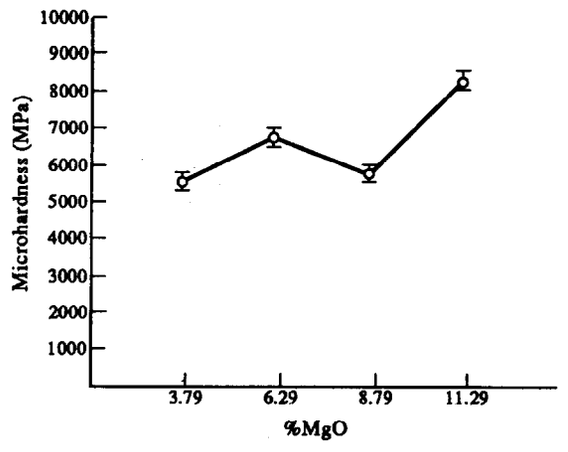

Fig. 9. Knoop hardness values versus composition (wt%). (Each point represents the average value for 3 specimens).

Table 5. Densities and porosities of crystallized specimens

	Specimen			
	B	*C*	*D*	*E*
Bulk density (Mgm^{-3})	2·73	2·97	2·81	2·85
Powder density (Mgm^{-3})	2·77	3·04	2·85	3·12
Total porosity (%) (Calculated)	1·44	2·63	1·40	8·65

Table 6. Chemical durabilities of glass-ceramics

Specimen	*Weight loss in NaOH* $Mgm^{-2} \times 10^{-5}$	*Weight loss*[a] *in HCL* $Mgm^{-2} \times 10^{-5}$
B	Negligible	125·97
C	Negligible	43·61
D	Negligible	85·11
E	Negligible	25·03

[a] Average values for 3 specimens.

were performed at pore-free regions of specimens under a weight of 500 g.) Each point represents the average value for three specimens.

3.5 Chemical durability

Table 6 shows the results of chemical durability of specimens after crystallization. Chemical durabilities were determined by weight loss of polished samples after immersion in 5% NaOH and 5% HCl solutions at 95°C for 24 h.

It is apparent that the resistance to acids is also a function of the crystallinity of material. Specimen E which has the highest amount of crystalline phase shows the highest resistance to acids.

4 Conclusions

Useful glass-ceramic materials can be made by using andesite rock as the primary raw material together with some lime, silica and MgO additions. Chromite ore 1 wt% is sufficient to induce glass in glass phase separation which is a precursor to nucleation in these glasses. A mixed spinel phase precipitating from a chromium rich phase after phase separation, probably acts as a nucleation agent. The replacement of CaO by MgO has a marked effect on the crystallization behaviour of glass compositions studied. There exists an optimum amount of MgO which gives rise to the highest amount of crystalline phase in a standard two stage heat treatment schedule. Although the physical and chemical properties of these glass-ceramic materials generally improve with their degree of crystallinity, the specimen with the highest amount of crystalline phase is not necessarily the strongest one. Specimen C which is almost 80%

crystalline exhibits the highest bending strength. It also possesses acceptable values for hardness and chemical durability and can be used as a suitable, inexpensive construction material.

References

1. Davies, M. W., Kerrison, B., Gross, W. E., Robson, M. J. & Wichall, D. F., Slag ceramics: a glass ceramic from blast-furnace slag. *J. Iron steel Inst.*, **208** (1970) 348–70.
2. Pincus, A. G., Soviet building with slag sitall. *Glass. Ind.*, **53** (1972) 6–9.
3. Hazeldean, G. S. F. & Wichall, D. F., Effect of chemical composition on nucleation and crystallization of slag-based glass-ceramics. *J. Iron steel Inst.*, **211** (1973) 574–80.
4. Topping, J. A., The fabrication of glass-ceramic materials based on blast furnace slag–A review. *J. Can. Ceram. Soc.*, **45** (1976) 63–7.
5. Beall, G. H. & Rittler, H. L., Basalt glass ceramics. *Am. Ceram. Soc. Bull.*, **55** (1976) 579–82.
6. Bahl, D., Roberts, J. A. & Weymouth, J. H., Basalt glass ceramics. *J. Aust. Ceram. Soc.*, **74** (1974) 25–7.
7. Hidalgo, M., Callejas, P. & Rincon, J. M., Microstructure characterization of basalt glass-ceramics. *Mater. Sci. Res.*, **21** (1987) 117–126.
8. Shelestak, L. J., Chavez R. A. & Mackenzie, J. D., Glass & glass ceramics from naturally occuring CaO–MgO–Al_2O_3–SiO_2 Materials. (I) Glass formation & properties. *J. Non-cryst. sol.*, **27** (1978) 75–81; 83–97.
9. Strnad, Z., Glass-ceramic Materials, Elsevier, New York, 1986, p. 112.
10. Coenen, M., Proceedings of the UCDV Conf., Scheweningen, 1965, p. 413.
11. Ohlberg, S. M. & Strickler, D. W., Determination of percent crystallinity of partly devitrified glass by X-ray diffraction. *J. Am. Ceram. Soc.* **45** (1962), 170–2.
12. Kim, H. S., Rawlings, R. D. & Rogers, P. S., Quantitative determination of crystalline and amorphous phases in glass–ceramics by X-ray diffraction analysis. *Br. Ceram. Trans. J.*, **88** (1989) 21–5.
13. McMillan, P. W., Glass-ceramics, 2nd edn., Academic Press, London, 1979, p. 81.